# Development of an Ultra-Compact High-Voltage DC-DC Converter for Modular Sensor Systems

Dincer Sirkeci, Martin Hempel, Lukas Adrian Bernert, Martin Schneider-Ramelow, Ulrike Ganesh
TU Berlin & Fraunhofer IZM
Gustav-Meyer-Allee 25
Berlin 13355
Ph: +49 30 46403-109; Fax: +49 30 46403-161
Email: dincer.sirkeci@tu-berlin.de

## Abstract

This paper presents the development and miniaturization of a high-voltage DC-DC converter module designed to power FPGA (**Field Programmable Gate Array)** units and sensor nodes in next generation seismic streamer systems for marine seabed analysis. The module converts a fixed input voltage of 120 V into two regulated output voltages of 12 V and 3.3 V, enabling decentralized power supply along the streamer sections. A cascaded topology using two buck converters was selected based on efficiency and thermal performance simulations with PSpice. Initial validation was conducted on prototype boards, followed by the implementation of a miniaturization concept through embedding active and passive components into the PCB's dielectric layers. The embedded module was designed with an opening in the center to give room for passing cables as the strain relief and data/power lines. The size of the module is limited by the diameter of the stream to ≤3.5 cm. Electrical measurements confirmed a reliable performance with efficiencies of up to 77.9%, supporting the suitability of the concept for future integration into the next-generation seismic ocean streamer.

## Key words

Buck converter, DC-DC converter, embedded PCB, high voltage, miniaturization, seismic streamer

## I. Introduction

Modern underwater sensing systems, such as seismic streamers, are essential tools for high-resolution mapping of the seabed. These systems play a critical role in applications like offshore wind farm foundation planning and geological exploration. The streamer is pulled by a vessel. A powerful sound source is attached to the beginning of the streamer. This generates a sound wave every second, which hits the seabed and is refracted and reflected back by inhomogeneities. These reflected sound waves are picked up by a large number of broadband microphones in the streamer, see Figure 1. To meet the increasing demands for spatial resolution and system flexibility, next-generation streamers must integrate more sensor nodes and processing units into tighter spaces, all while maintaining a lightweight, robust, and modular design. A major engineering challenge in such systems is the distribution of electrical power along cable lengths of several hundred meters. Low supply voltages result in high currents, which in turn lead to significant line losses and the need for thick, heavy conductors. To overcome this, a centralized high-voltage supply (e.g., 120 V) is used, and local voltage conversion is performed directly withing each streamer segment. This paper presents the design and realization of a highly compact DC-DC converter module, developed specifically for integration into a 3.5-cm diameter streamer segment.

Compared to state-of-the-art high-voltage power modules used in seismic streamers and similar distributed sensing applications, the proposed design employs advanced 3D integration through PCB embedding to achieve substantial miniaturization and improved performance. While conventional modules often rely on discrete PCB assembly with larger footprints and higher weight, embedding active and passive components within the PCB dielectric layers enables a nearly 60% size reduction and an almost 90% weight reduction without compromising electrical efficiency.

In addition, the integration of all components directly into the PCB significantly enhances mechanical robustness and long-term reliability by eliminating solder joint stress and reducing vulnerability to vibration and environmental influences compared to conventional state-of-the-art solutions. The converter transforms a 120 V input into regulated 12 V and 3.3 V outputs to supply FPGA-based data processing units and sensor nodes. The module is miniaturized using an embedded PCB approach, allowing both passive and active components to be integrated into the dielectric inner layers of the board. Simulation, prototyping, fabrication, and measurement results are presented to validate the approach and demonstrate its suitability for field deployment in ultra-high-resolution sensor platforms.

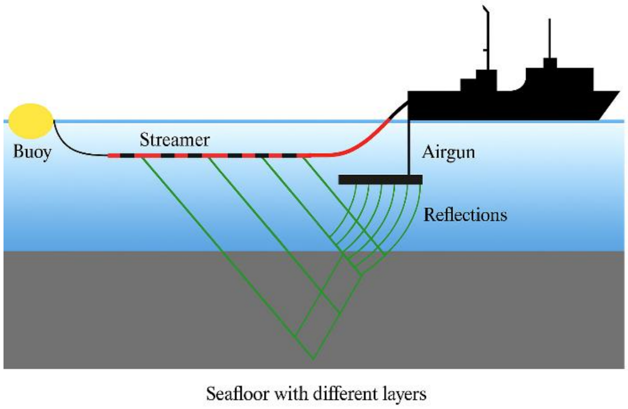


*Figure 1 Operating principle of a towed streamer system for underwater acoustic measurements.*

## II. Converter Design and Implementation

*A. Experimental*

The converter module developed in this work is designed for use in the Next-GEN-UHR-Streamer platform, a modular underwater sensor system used for high-resolution geological seabed analysis. Each streamer consists of up to twenty 25 m long sections, which are further divided into 2 m long internal segments. Each segment includes four sensor nodes with eight microphones each and one FPGA-based data aggregation unit. To enable autonomous, distributed operation, each segment requires local power conversion from a high-voltage line supply. To minimize voltage, drop and power losses over the total streamer length of up to 500 m, a high input voltage of 120 V DC was chosen for the centralized power distribution. This reduces the required current at each segment, as defined by:

$$I = \frac{P}{U} \quad (1)$$

Reducing the current also minimizes power dissipation in the cable, which is described by:

$$P_{loss} = I^2 \cdot R \quad (2)$$

A lower current allows for thinner and lighter wires, which is essential to ensure the streamer remains neutrally buoyant and flexible. Local power conversion is necessary to supply the required voltages of 12 V and 3.3 V for the FPGA and sensor nodes. The power consumption per segment is approximately 8 W for the FPGA and 1 W per one of the four sensor nodes, resulting in a total of 12 W per segment. To meet strict spatial constraints – particularly a maximum outer diameter of 3.5 cm and the need for a central opening – the converter module was developed with a circular layout and central cutout, enabling mechanical and signal routing through the center. A cascaded converter topology was selected, consisting of:

- A first – stage buck converter: 120 V to 12 V
- A second – stage buck converter: 12 V to 3.3 V

This architecture offers high efficiency and allows for optimal component dimensioning. Simulation and circuit validation were initially performed using discrete components, followed by miniaturized embedded PCB implementation [1] to meet the dimensional and integration requirements.

*B. Simulation and Prototyping*

To verify the converter architecture and ensure the desired power output, detailed simulations were performed for both the 120 V to 12 V and the 12 V to 3.3 V converter stages using PSpice [11]. These simulations were based on theoretical calculations and real component models, and were used to optimize the switching behavior, ripple, and sizing of passive components.

**Buck Converter: 120 V to 12 V**

The output current for the first stage was calculated using:

$$I_{Out,12V} = \frac{P_{Out}}{U_{Out}} = \frac{8\,W}{12\,V} = 666.7\,mA \quad (3)$$

With a switching frequency $f_s = 100\,kHz$, the period $T$ is:

$$T = \frac{1}{f_s} = 10\,\mu s \quad (4)$$

The duty cycle $D$ is:

$$D = \frac{U_{Out}}{U_{In}} = \frac{12\,V}{120\,V} = 0.1 \quad (5)$$

The minimum inductance was calculated to limit current ripple to 10% of the output current:

$$L_{min} = \frac{U_{Out} \cdot T}{2 \cdot I_{Out} \cdot (1-D)} = \frac{12\ V \cdot 10\ \mu s}{2 \cdot 0.7\ A \cdot (1-0.1)} = 66.7\ \mu H \quad (6)$$

The output voltage ripple was kept below 1 % of the nominal output:

$$\Delta U = 1\% \cdot U_{Out} = 0.12\ V \quad (7)$$

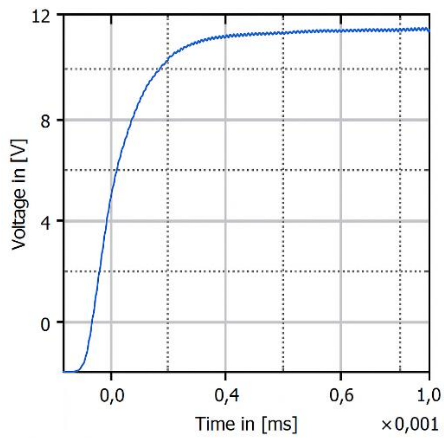


*Figure 2 Simulated output voltage of the first-stage buck converter (120 V to 12 V).*

Figure 2 shows a stabilized output voltage of 11.65 V after ~630 µs and a voltage ripple of 0.1 V, corresponding to 0.86 %, which is within acceptable limits. The output current reaches 777 mA with minimal ripple.

**Buck Converter: 120 V to 3.3 V (Cascade):**

Initial attempts to convert 120 V directly to 3.3 V using a single-stage buck converter revealed that the required duty cycle was extremely low, resulting in a switching delay that exceeded the recommended limits. This led to increased switching losses and unstable output behavior. Alternatives such as lowering the switching frequency would have required significantly larger passive components, conflicting with the strict miniaturization constraints of the system. To overcome these challenges, a cascaded topology was selected. By splitting the voltage conversion into two stages—first from 120 V to 12 V, and then from 12 V to 3.3 V—the voltage difference per stage was significantly reduced. This minimized the switching losses and allowed the use of smaller, more efficient components. Although the module provides both 12 V and 3.3 V outputs, only one output is used at a time, depending on the application. The switching frequency remains at 100 kHz, ensuring compatibility with earlier designs.

$$I_{Out,3,3V} = \frac{8\ W}{3,3\ V} = 2.42\ A \quad (8)$$

$$D = \frac{U_{Out}}{U_{In}} = \frac{3,3\ V}{12\ V} = 0.275 \quad (9)$$

Due to the lower voltage and higher current, the required inductance is smaller:

$$L_{min} = \frac{U_{Out} \cdot T}{2 \cdot I_{Out} \cdot (1-D)} = \frac{3.3\ V \cdot 10\ \mu s}{2 \cdot 2.5\ A} \cdot (1-0.275) = 4.785\ \mu H \quad (10)$$

To achieve only 10% current ripple, a higher inductance was considered:

$$L_{10\%} = \frac{(U_{In} - U_{Out)} \cdot t_{On}}{\Delta I} = \frac{1}{250\ mA} \cdot (12\ V - 3.3\ V) \cdot 2.75\ \mu s = 95.7\ \mu H \quad (11)$$

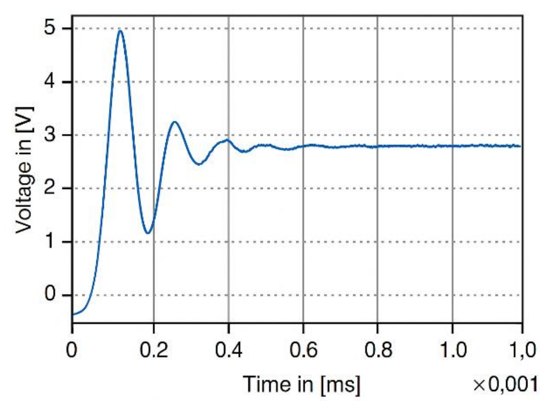


*Figure 3 Simulated output voltage of the second-stage buck converter (120 V to 3.3 V).*

Figure 3 shows the simulation results. The output stabilizes at approximately 3 V after around 0.7 ms, following initial overshoot and oscillations due to switching delays. The steady-state ripple remains within acceptable limits for typical logic-level applications.
All calculations were based on established methods documented in existing technical literature [7].

**Prototyping:**

To validate the simulation results and assess the practical feasibility of the converter design, a discrete prototype was developed. The prototyping phase included separate test PCBs for the 120 V to 12 V stage, the 12 V to 3.3 V stage, and the associated filtering and protection circuits. Components were selected to match the simulation parameters, and the prototype was assembled using standard SMD and through-hole techniques. To ensure stable startup and low conducted emissions, an EMI filter was placed at the input stage. It consisted of common-mode chokes and decoupling capacitors to suppress high-frequency noise generated by the switching converters. Additionally, a diode-ORing circuit was implemented at the output to allow automatic selection between the 12 V and 3.3 V output, depending on the connected load. This ensured that only one voltage path was active at a time, preventing backfeed and simplifying the system integration. For testing, the input voltage was supplied via a laboratory power source.

The 3.3 V output stage was connected to a resistive load of R=1.2 Ω, corresponding to a load current of approximately 2.75 A. The measured output voltage stabilized at 3.29 V, and the load current reached 2.63 A, resulting in an effective output power of 8.6 W. The measurements confirmed correct startup behavior, good voltage regulation, and overall stable operation. Minor deviations in ripple and transient response were observed, attributed to switching delays and parasitic elements. Nevertheless, the prototype validated the cascaded converter architecture and its suitability for further miniaturization in an embedded PCB implementation.

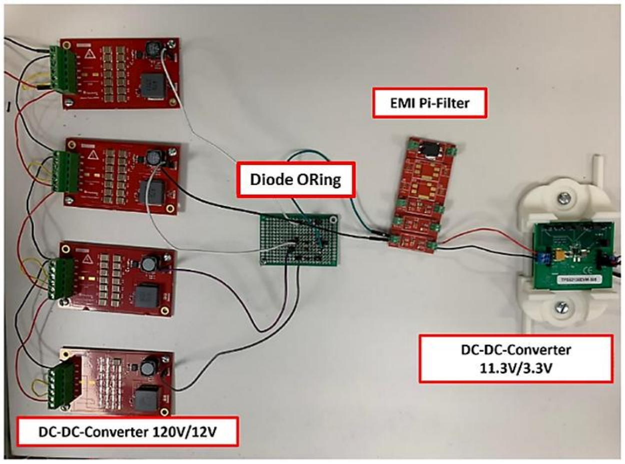


*Figure 4 Integration of the individual prototype boards.*

The prototype setup was successfully assembled, and practical measurements were carried out under realistic load conditions. The results of these measurements are presented and discussed in detail in E – Electrical Characterization.

### *C. Embedded PCB Miniaturization*

After successful validation of the converter prototype, the next step involved the miniaturization and integration of the power electronics into an embedded PCB module. Due to strict mechanical constraints within the streamer system — specifically a maximum outer diameter of 3.5 cm and the need for a central opening — a conventional PCB assembly was not feasible. Therefore, an embedded design approach was adopted to integrate both passive and active components directly into the inner layers of the PCB. The layout was realized as a circular module with a central cutout to accommodate the mechanical core, which carries the load-bearing structure as well as combined power and data lines. These constraints imposed strict geometrical requirements and limited available space for component placement. The design was implemented across multiple PCB layers, using dedicated copper layers for signal and power routing and electro-magnetic shielding, and internal cavities for embedding the components.

The embedding concept and PCB build-up were realized at Fraunhofer IZM, based on existing in-house know-how and established process technologies. The corresponding methods and references can be accessed in Refs. [1].

Key challenges in the embedded implementation included:

- **Component selection for low profile** and thermal compatibility
- **Precise placement and alignment** of embedded chips and inductors
- **Thermal path optimization** to avoid hotspots during continuous operation

The module was manufactured using an industrial embedding process. Each layer was fabricated, stacked, and laminated under controlled temperature and pressure. The embedded components were electrically connected using vias and surface pads. An additional routing layer was used to connect measurement and test points. Initial visual inspections, height measurements, and X-ray imaging confirmed proper embedding, alignment, and bonding of all components. The final module fulfilled all geometric constraints, enabling seamless integration into the streamer prototype for further electrical testing.

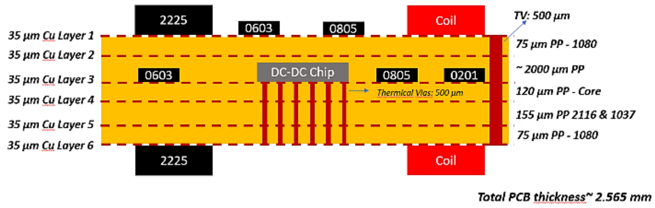


*Figure 5 Stack-up of the DC-DC converter module.*

The structure consists of a six-layer PCB with 35 µm copper thickness per layer. A DC-DC converter chip (LM5168PQDDARQ1) [5] and several passive components are integrated within the board. Figure 6 shows the 3D CAD model. The passive components include standard surface-mount device (SMD) packages such as 0603, 0805, 0201, and 2225, which refer to components of different sizes.

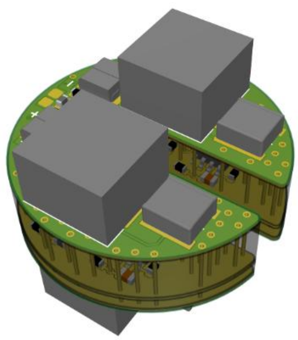

*Figure 6 3D model of the embedded DC-DC converter, stretched in z-direction for better visibility.*

## D. Fabrication Process

This section describes the fabrication process of the embedded DC-DC converter module, focusing on the integration of active and passive components within a multilayer PCB using a miniaturized build-up approach.

*Figure 7 Inner layer of the embedded DC-DC converter module.*

The SMD components were placed into the milled cavities of the core using adhesive and alignment tools, Figure 7. Afterwards, the PCB was laminated under high pressure and temperature. This step permanently sealed the embedded components between dielectric layers while ensuring mechanical stability. X-ray imaging and height measurement were performed post-lamination to verify correct component positioning and planarity. As shown in Figure 8, these analyses confirmed that all embedded components were properly aligned and the overall structure remained planar.

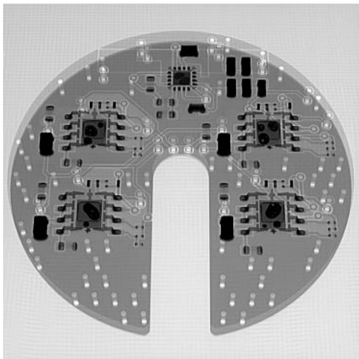

*Figure 8 X-ray imaging for embedded component verification.*

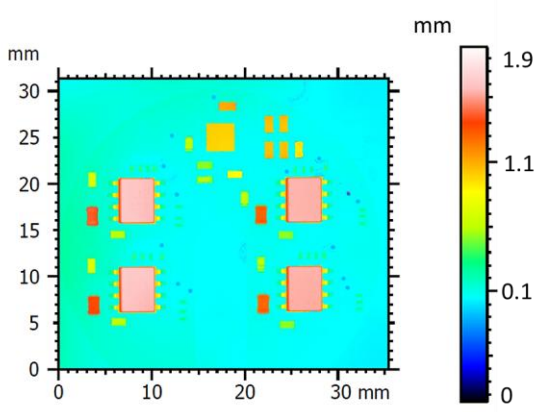


*Figure 9 Component height measurement.*

To determine the exact component heights within the inner layer, a surface profile measurement was carried out. Based on the results, the PCB stack-up was adapted accordingly. Figure 9 shows the measured height distribution of the embedded components.


*Figure 10 Component placement on the outer layer.*

Figure 10 shows the outer layer of the PCB, where inductors and other large components were assembled. Due to their height, these components could not be embedded within the multilayer structure and were instead mounted on the surface and electrically contacted externally.

### *E. Electrical Characterization*

The electrical performance of the cascaded DC-DC converter module was evaluated under controlled laboratory conditions. A GW Instek GPP-4323 precision DC power supply provided a stable input voltage in the range of 40 V to 120 V, with a regulated 120 V input applied to the converter's terminals during testing. The output was connected to resistive loads simulating real application conditions. For the 3.3 V output stage, a resistive load of $R = 1.2\,\Omega$ was used, resulting in a measured output voltage of 3.29 V and a corresponding load current of 2.63 A, yielding an output power of 8.6 W. Output voltage and current were recorded using a Keysight U1282A true RMS multimeter, while ripple and transient behavior were captured with a RIGOL DS1054Z digital oscilloscope. The measured ripple voltage remained within acceptable limits and showed good agreement with simulated values. Transient measurements during startup revealed a stable voltage settling within approximately 700 µs. For consistency and comparability, the same instruments and procedures were applied during the characterization of both the discrete prototype and the embedded module.

| Output Current [A] | Output Voltage [V] | Output Power [W] |
|---|---|---|
| 2.63 A | 3.29 | 8.6 |

*Table 1 Output voltage and current of the prototype board setup*

The 12-V output stage was tested separately using an equivalent setup. At nominal load, the converter delivered 11.68 V with an output current of 790 mA, confirming functional stability and low voltage deviation under load.

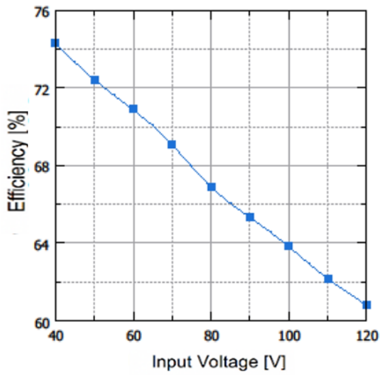


*Figure 11 Measured efficiency of the discrete test module as a function of input voltage.*

To evaluate the performance of the miniaturized embedded DC-DC converter module, various electrical measurements were conducted. The input voltage was varied from 40 V to 120 V, and the corresponding input current, input power, output power, and efficiency were recorded. The converter was configured to deliver 3.3 V at a load current of approximately 2.7 A, resulting in an output power of 8.91 W. The results demonstrate that the efficiency peaks at 84.05% at 40 V input and gradually decreases to 61.88% at 120 V input. This drop in efficiency at higher voltages is primarily attributed to increased switching losses and thermal stress in the converter ICs. Figure 12 illustrates the efficiency curve of the embedded module across the input:

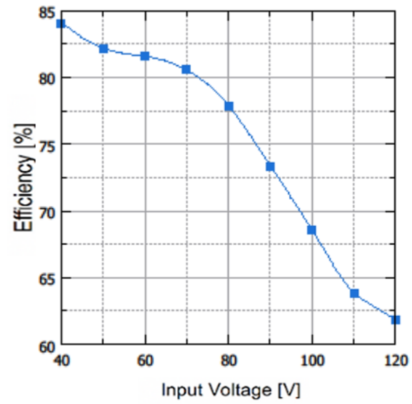


*Figure 12 Measured efficiency of the embedded DC-DC converter module as a function of input voltage.*

### *F. Discussion*

The measurement results confirm the functional reliability of both the discrete prototype setup and the final embedded DC-DC converter module. However, a clear distinction can be observed in terms of electrical efficiency and physical integration. Although the prototype boards performed well, the embedded module showed improved energy conversion efficiency across most of the input voltage range. At 40 V input, the embedded module achieved an efficiency of 84.05%, whereas the discrete setup reached only 75.55%. This improvement is primarily attributed to the shorter interconnects, reduced parasitic losses, and optimized thermal paths enabled by the embedding technology. At higher voltages, both systems exhibit decreasing efficiency due to increased switching losses, but the embedded module consistently outperforms the prototype. Beyond electrical performance, the advantages of the miniaturization process are clearly visible in terms of size and weight. Nevertheless, both designs show a noticeable drop in efficiency at higher input voltages (above ~80 V), mainly due to increased switching losses and thermal stress in the converter IC. Potential improvements include optimizing thermal management through additional thermal vias and copper heat-spreading layers, selecting MOSFETs with lower gate charge and on-resistance, and refining the PCB layout to minimize parasitic inductance and capacitance. These measures can help sustain higher efficiency across the entire input voltage range in future designs.

| Module | Area [mm²] | Weight[g] |
|---|---|---|
| 12 V Converter | 4872.385 | 47.7 |
| 12 V Combined | 19489.54 | 190.8 |
| Diode-ORing | 1227.32 | 10.9 |
| EMI Filter | 478.59 | 15.2 |
| 3.3 V Converter | 2829.06 | 17.2 |
| Total | 24024.54 | 234.1 |
| | | |
| Embedded Module | 9621 | 26 |
| Difference | 14403.54 | 208.1 |
| | 59.95% smaller | 88.89% lighter |

*Table 2 Size and weight comparison between the discrete prototype board setup and the embedded DC-DC converter module.*

Table 2 shows that the embedded module requires 59.95% less board area and is 88.89% lighter compared to the combined prototype boards. This dramatic reduction was achieved by consolidating all functional stages—12 V and 3.3 V converters, EMI filter, and diode-ORing—into a single multilayer PCB using component embedding.

These results demonstrate that the embedded converter not only meets the electrical requirements but also offers significant benefits in mechanical integration. The reduced volume and weight are especially beneficial for applications with space and mass constraints, such as modular sensor systems or mobile platforms.

## III. Conclusion

This paper presents the development, prototyping, and miniaturization of a cascaded high-voltage DC-DC converter designed to supply 12 V and 3.3 V outputs from a 120 V input, targeting integration into compact embedded systems. Simulation and prototyping confirmed the electrical functionality of the cascaded topology, while measurements revealed stable voltage regulation and efficient operation across a wide input voltage range from 40 V to 120 V. The transition from discrete prototype boards to an embedded multilayer PCB enabled a significant reduction in both physical size and weight by 59.95% and 88.89%, respectively, while maintaining or even improving electrical efficiency. The embedded module achieved a peak efficiency of 84.05% (Input Voltage: 40V) and offered better thermal and electromagnetic behavior due to the optimized layout and shorter interconnect paths. These results demonstrate the technical viability of using embedded power electronics for high-voltage applications with stringent space constraints. The successful implementation highlights the potential of advanced PCB embedding technologies in future miniaturized sensor and converter systems, especially in fields such as marine sensing, mobile electronics, and distributed measurement platforms. This work also exemplifies the concept of heterogeneous integration by combining high-voltage power conversion, electromagnetic filtering, and mechanical integration within a single embedded PCB module. Such integration reduces interconnect complexity, improves mechanical robustness, and enhances long-term reliability compared to conventional multi-board solutions.

## Acknowledgment

The authors would like to acknowledge the valuable technical support provided during the development, fabrication, and testing of the converter system. The contributions made in the areas of PCB embedding, measurement setup, and simulation were essential to the successful realization of this work. The authors also appreciate the access to laboratory equipment and facilities that enabled the practical validation of the developed module. This work was carried out as part of the NEXT GENERATION ULTRA-HIGH-RESOLUTION SEISMIC STREAMER project.

## References

[1] T. Loher, D. Schütze, M. Spanier, A. Ostmann, and M. Schneider-Ramelow, “PCB Embedding Technology for the Miniaturization of complex electronic systems,” 2022 IEEE CPMT Symposium Japan (ICSJ), 11 2022.
[2] N. D. Manessis, N. L. Boettcher, N. A. Ostmann, N. S. Karaszkiewicz, and N. H. Reichl, “Breakthroughs in chip embedding technologies leading to the emergence of further miniaturized system-in-packages,” 2009 4th International Microsystems, Packaging, Assembly and Circuits Technology Conference, pp. 174–177, 10 2009.
[3] D. Manessis, L. Boettcher, S. Karaszkiewicz, A. Ostmann, R. Aschenbrenner, and K.-d. Lang, “Chip embedding technology developments leading to the emergence of miniaturized system-in-packages,” European Microelectronics and Packaging Conference, pp. 1–8, 9 2011.
[4] D. Schutze, M. Voitel, S. Gottwald, M. Spanier, K.-F. Becker, A. Ostmann, T. Loher, A. Hofmeister, and M. Schneider-Ramelow, “Miniaturized Sensor Modules for under Water Applications realized by Printed Circuit Board Embedding Technology,” 2022 IEEE 9th Electronics System-Integration Technology Conference (ESTC), pp. 49–54, 9 2022.J.
[5] Texas Instruments, LM5168PEVM EVM User’s Guide. Texas Instruments, Dallas, Texas, USA, August 2022. User’s Guide, SNVU826.
[6] Texas Instruments, LM516x, 0.65A/0.3A, 120V Absolute Maximum, Step-Down Converter With Fly-Buck Converter Capability, rev. b ed., Dec. 2024. Datasheet for LM5168 and LM5169, Texas Instruments.
[7] U. Tietze, C. Schenk, and E. Gamm, Halbleiter-Schaltungstechnik. Springer Vieweg, 7 2019.
[8] U. Probst, Leistungselektronik für Bachelors. 4 2022.
[9] F. Zach, Leistungselektronik. Springer Vieweg Wiesbaden, 6 ed., 2022. Springer Fachmedien Wiesbaden GmbH, ein Teil von Springer Nature.
[10] ProtoSupplies, “Dc-dc step down converter overview,” 2023.
[11] https://www.ti.com/tool/de-de/PSPICE-FOR-TI